Available online at www.sciencedirect.com
SCIENCE DIRECT®
ELSEVIER
Journal of Nuclear Materials 346 (2005) 293–297
journal of nuclear materials
www.elsevier.com/locate/jnucmat

Hydrogen diffusion in liquid lithium from 500 °C to 650 °C

S. Fukada [a,*], M. Kinoshita [b], K. Kuroki [b], T. Muroga [c]

[a] *Department of Applied Quantum Physics and Nuclear Engineering, Kyushu University, 6-10-1, Hakozaki, Higashi-ku, Fukuoka 812-8581, Japan*
[b] *Department of Advanced Energy Engineering Science, Kyushu University, Fukuoka 812-8581, Japan*
[c] *Fusion Engineering Research Center, National Institute of Fusion Sciences, Toki 509-5292, Japan*

Received 22 February 2005; accepted 30 June 2005

Abstract

In order to provide data for designing an Y hot trap to recover tritium from flowing liquid Li, diffusion coefficients and solubility constants of hydrogen in Li were determined with a capillary method between 500 °C and 650 °C. The diffusivity of hydrogen in Li determined here were correlated to $D_{\mathrm{Li-H}} = 1.38\exp(-162[\mathrm{kJ/mol}]/R_gT)$. The correlation was consistent with one extrapolated from the previous Alire's correlation at higher temperature. Discrepancies among other previous diffusivity data were discussed in terms of the interaction of Li with H. The solubility determined was consistent with values extrapolated from the previous Sieverts' constant by Veleckis et al.

PACS: 61.25.Mv; 66.10.−x

1. Introduction

In order to generate a materials irradiation database for a fusion demonstration reactor, a facility of an intensive neutron source called IFMIF (International Fusion Materials Irradiation Facility) is being designed in a joint effort of EU, Japan, the Russian Federation and USA [1,2]. IFMIF is identified as the most appropriate machine to provide fusion relevant neutron environment in order to develop low activation materials for fusion reactors. In the liquid Li target loop of IFMIF, around 7 g/year tritium will be generated as a by-product by neutron from *D*-Li stripping reactions [3]. The technique of cold trapping and hot trapping was proposed for the removal of nitrogen, carbon, oxygen and tritium in the flowing liquid Li. Metallic Y is considered the most promising material for the hot trap to remove tritium. The diffusivity of tritium in Li is a crucial factor to determine the capacity and operating conditions of an Y bed to remove tritium dissolved in Li. This is because diffusion of tritium in Li is considered a rate-controlling step in the Li–Y–tritium system [4,5].

Two experimental data were available on diffusivity in liquid Li at temperatures higher than 500 °C [6,7]. They were determined by means of two different techniques. The way by Alire [6] was based on measuring hydrogen transport through Li enclosed in a Nb/1% Zr container. That by Moriyama et al. [7] was based on detecting rates of tritium diffusing through a fresh Li reservoir attached to irradiated Li. However, there were large discrepancies between their diffusivity data. Moreover, there were few data at temperatures around

---

[*] Corresponding author. Present address: 6-10-1 Hakozaki, Higashi-ku, Fukuoka 812-8581, Japan. Tel.: +81 92 642 4140; fax: +81 92 642 3800.
E-mail address: sfukada@nucl.kyushu-u.ac.jp (S. Fukada).

0022-3115/$ - see front matter © 2005 Elsevier B.V. All rights reserved.
doi:10.1016/j.jnucmat.2005.06.021

500 °C, which is the typical operating condition of the Li purification system of IFMIF. In the present study, we determined the diffusivity and solubility of hydrogen in Li by a capillary method between 500 °C and 650 °C to provide design data for an Y hot bed inside the IFMIF Li loop. The achieved results were compared with previous diffusivity and solubility data.

2. Experiment and analysis

2.1. Experimental apparatus and procedures

Fig. 1 shows a schematic diagram of the experimental apparatus used in the present study. The stated purity of Li used here was 99.9%. Impurities included in Li before use were Na 200 ppm, K 100 ppm, Ca 500 ppm, Fe 20 ppm, Si 100 ppm and others less than 100 ppm including carbon, oxygen, nitrogen and hydrogen. The last non-metallic impurities will be included also under the operating condition of IFMIF. The solid Li was packed in a 316 stainless-steel capillary tube with inner diameter of 4.35 mm and with thickness of 1.00 mm in an Ar atmosphere glove-box that can be evacuated by a vacuum pump. The length of the Li layer in the capillary tube was 2.0 cm or 3.0 cm. We melted the solid Li by heating to 500 °C under a highly purified Ar flowing condition, where research grade Ar with stated purity 99.9999% was further purified through a bed packed with SAES getter ST707 (Zr–V–Fe alloy) to remove gaseous impurities. We continued to blow fresh Ar into the both ends of the capillary tube until the hydrogen concentrations of the upstream and downstream sides of the Li layer became lower than 1 vppm. The outside of the capillary tube was evacuated by means of a turbomolecular pump. Bypass permeation through the stainless-steel tube was found to be negligibly small, because H permeability through Li was around thousands times higher than that of 316 stainless-steel.

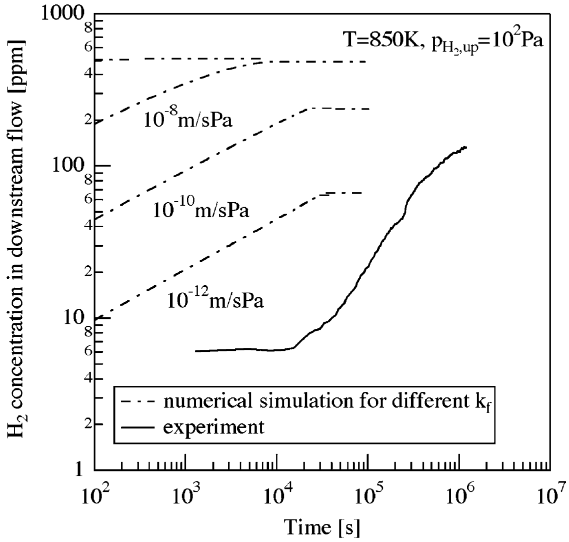

Fig. 1. A schematic diagram of the experimental apparatus to measure diffusion of hydrogen in Li.

After the confirmation of zero hydrogen concentration in the downstream and upstream sides, a purified H_2–Ar gas mixture was introduced to the upstream side through a six-way valve. At the same time purified Ar was blown into the downstream side. The hydrogen concentration in the upstream side was 100 vppm or 1000 vppm. Hydrogen permeating through Li was swept out by the downstream Ar flow. The hydrogen concentration of the downstream side was detected by gas chromatography with the detection limit of 0.2 vppm. The gas flow rates of Ar and Ar–H_2 were controlled to 5.0 cm^3(NTP)/min by mass-flow controllers. The effect of Li vaporization was negligibly small in this experimental condition. The Li–H system under the present experimental conditions was always in the α-phase judging from the Li–H phase diagram [8]. The Li layer and the capillary tube after each experimental run were exchanged with new ones.

2.2. Analysis

Experimental data were analyzed by a one-dimensional diffusion equation as follows:

$$\frac{\partial c}{\partial t} = D_{\text{Li–H}} \frac{\partial^2 c}{\partial x^2}. \tag{1}$$

The initial and boundary conditions are as follows:

$$t = 0 \quad c = 0 \tag{2}$$

$$x = 0 \quad -D_{\text{Li–H}} \frac{\partial c}{\partial x} = k_f \left(p_{H_2,\text{up}} (1 - c_{\text{up}})^2 - \frac{c_{\text{up}}^2}{K_{\text{Li–H}}} \right) \tag{3}$$

$$x = L \quad -D_{\text{Li–H}} \frac{\partial c}{\partial x} = k_f \left(p_{H_2,\text{down}} (1 - c_{\text{down}})^2 - \frac{c_{\text{down}}^2}{K_{\text{Li–H}}} \right). \tag{4}$$

Here, c is the local hydrogen atom ratio (H/Li) in the Li layer with the Li length of L, $D_{\text{Li–H}}$, $K_{\text{Li–H}}$ and k_f are the diffusivity and solubility of H in Li and the reaction-rate constant, and $p_{H_2,\text{up}}$ and $p_{H_2,\text{down}}$ are the hydrogen partial pressures at the surfaces of the upstream and downstream sides. In addition to Eq. (4), a purge condition is applied to the downstream flow as follows:

$$-AD_{\text{Li–H}} \left. \frac{\partial c}{\partial x} \right|_{x=L} = \frac{W p_{H_2,\text{down}}}{2 p_t}. \tag{5}$$

Here, W is an Ar molar flow rate in the downstream side, p_t is a total pressure in the downstream side, and A is the surface area of the Li layer. The solution to

Eq. (1) under the initial and boundary conditions of Eqs. (2)–(5) was numerically obtained by means of a predictor–corrector method.

Chain lines in Fig. 2 show variations of $p_{H_2,down}$ with time for different k_f values and the same $D_{Li\text{–}H}$ value. The $D_{Li\text{–}H}$ value used for the calculation is the Moriyama's experimental data [7]. The variations of $p_{H_2,down}$ with time correspond to those of a hydrogen permeation flux through a Li layer. As seen in the figure, the variations of $p_{H_2,down}$ with time under any k_f values diverged remarkably from our experimental ones shown by a solid line in the figure. With the increase of k_f, the steady-state value of $p_{H_2,down}$ increased under the same $D_{Li\text{–}H}$ value. Thus, the parameter k_f affected only the steady-state $p_{H_2,down}$ value. The effect of k_f on overall hydrogen permeation rates became negligibly small when $k_f > 10^{-6}$ m/s Pa. The situation means that the rate-determining step is hydrogen diffusion in Li under the present experimental condition. Moreover, the transient behavior of $p_{H_2,down}$ did not change regardless of different k_f values. Consequently, the calculation result under the lower k_f values was not in agreement with the present experimental results at all. Therefore, it was concluded that the effect of the reaction-rate on upstream and downstream sides, i.e., reaction of dissociation and recombination, can be neglected under the present experimental conditions.

When k_f is large, the Li–H$_2$ interface approaches to an equilibrium condition. Then, the boundary conditions of the upstream and downstream sides, Eqs. (3) and (4), are reduced to the Sieverts' relation:

$$\text{at } x = 0, \quad c_{up}/(1 - c_{up}) = K_{Li\text{–}H}\, p_{H_2,up}^{0.5}, \tag{6}$$

$$\text{at } x = L, \quad c_{down}/(1 - c_{down}) = K_{Li\text{–}H}\, p_{H_2,down}^{0.5}. \tag{7}$$

Since c_{up} and c_{down} in the α-phase are much smaller than unity, the left-hand sides of Eqs. (6) and (7) are usually approximated to c_{up} and c_{down}.

The permeation mass flux through the downstream Li surface, j, changes from 0 to a steady-state value with time elapsing. The steady-state mass flux under the diffusion-limiting condition, j_0, is expressed as follows:

$$j_0 = \frac{D_{Li\text{–}H}K_{Li\text{–}H}}{L}\left(\sqrt{p_{H_2,up}} - \sqrt{p_{H_2,down}}\right). \tag{8}$$

If $p_{H_2,down}$ is much smaller than $p_{H_2,up}$, an analytical solution to Eq. (1) under a transient condition can be obtained. The hydrogen mass flow rate on the downstream surface is expressed under the diffusion-limiting condition as follows:

$$\frac{j}{j_0} = \sqrt{\frac{4L^2}{\pi D_{Li\text{–}H}t}}\sum_{n=0}^{\infty}\exp\left(-\frac{(2n+1)^2L^2}{4D_{Li\text{–}H}t}\right) \tag{9a}$$

$$\frac{j}{j_0} = 1 + 2\sum_{n=1}^{\infty}(-1)^n\exp\left(-\frac{n^2\pi^2D_{Li\text{–}H}t}{L^2}\right). \tag{9b}$$

Both of the two equations of Eqs. (9a) and (9b) are solutions to Eq. (1) under the diffusion-limiting condition. Eq. (9a) gives exact values with the small number of n for the case of small t. On the other hand, Eq. (9b), gave exact values with the small number of n for the case of large t. Here, j is a transient hydrogen permeation flux through the downstream Li surface. When t is very large, j approaches j_0. We determined the value of the product of $D_{Li\text{–}H}$ and $K_{Li\text{–}H}$ from the steady-state value of j_0, and the value of $D_{Li\text{–}H}$ from the transient curve of j independently.

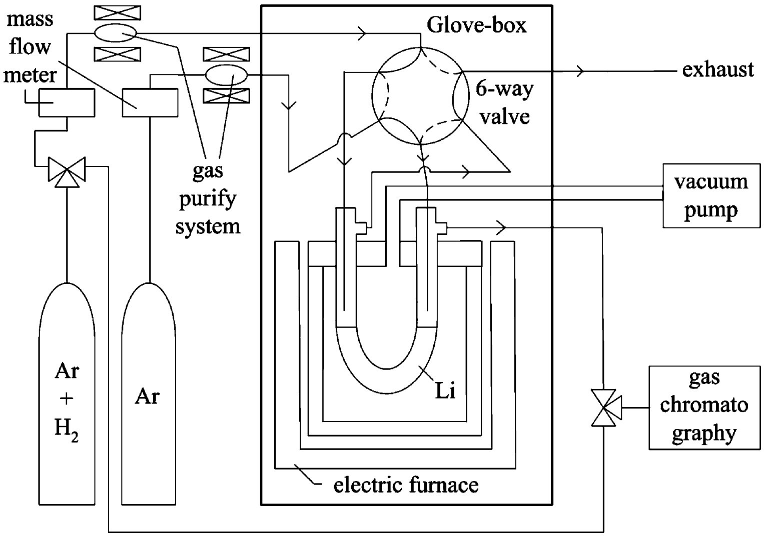

Fig. 2. Effects of reaction-rate constant on hydrogen permeation behavior.

3. Results and discussion

Fig. 3 shows variations of the H_2 concentration in the downstream Ar flow with time. The experimental variations were fitted by curves calculated by Eqs. (1), (2) and (5)–(7). Close agreement was obtained between the experiment and analysis for each temperature condition except for a very small time region. From fitting the experimental data to the analysis, the diffusivity and solubility were simultaneously determined from a $p_{H_2,\text{down}}$ curve. Disagreement was limited to the small t region. The disagreement might be because of background hydrogen less than 1 vppm. The background hydrogen was observed immediately after the H_2–Ar introduction as seen in the solid line of Fig. 2. When we distracted the background hydrogen concentration from the original experimental value, closer agreement was achieved, although not shown in the figure.

Fig. 4 shows a comparison of the values of diffusivity of H in Li determined here with previous experimental data. Our data were correlated to the following equation:

$$D_{\text{Li–H}} = 1.38 \exp\left(-\frac{162\ [\text{kJ/mol}]}{R_g T}\right) [\text{m}^2/\text{s}]. \tag{10}$$

This equation was near to an extrapolation line of the Alire's correlation [6]. However, there was much discrepancy between our data and Moriyama's ones [7]. For comparison, the self-diffusivity of the ^{6}Li–^{7}Li system [9] is also plotted in Fig. 4. Close agreement was obtained between Moriyama's data and the self-diffusivity of Li. In addition to that, the activation energy of the self-diffusivity of the ^{6}Li–^{7}Li system was near to that of the Li viscosity [10]. Judging from the Stokes–Einstein equation, these two facts strongly suggested that Li combined with tritium diffused in a similar way to Li without tritium. This result corresponds to the Moriyama's experiment. On the other hand, the activation energy of our data as well as Alire's ones was larger than that of the self-diffusivity of Li. This means that H atoms combined with Li diffuses from a site of metallic liquid Li to its neighbor site based on a hopping mechanism. In other words, H atoms jump from a Li–H site to a neighboring Li site over a high potential barrier. There might be two possible reasons to explain the high potential barrier: (i) effects of impurity included in Li such as oxygen or others, or (ii) effects of another surface reaction on the Li–H_2 interface. We could not determine where the higher potential barrier comes from.

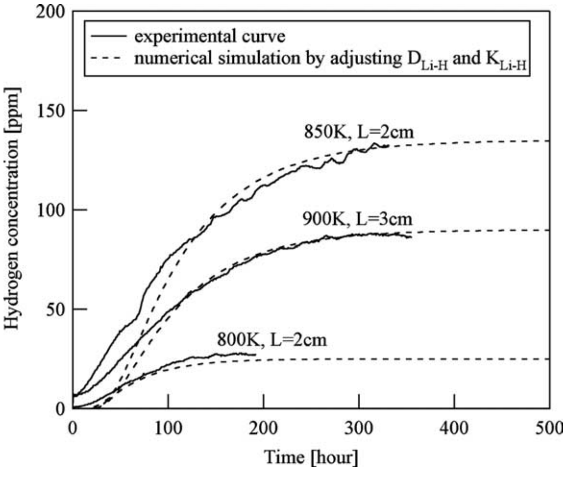

Fig. 3. Comparison of the H_2 concentration in the downstream between experiment and numerical calculation.

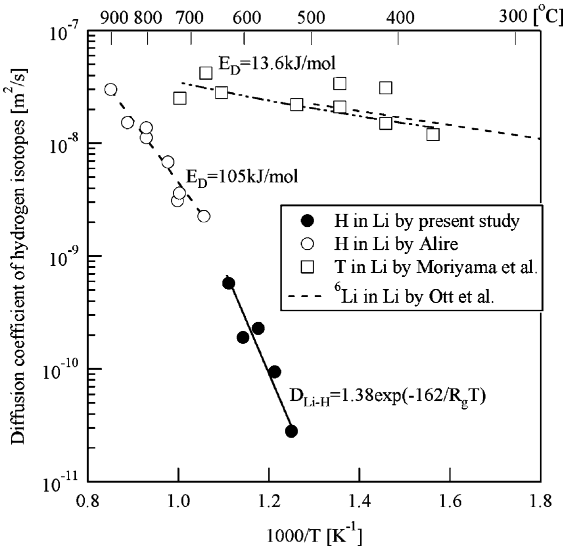

Fig. 4. Comparison of diffusivity between the present study and previous ones.

Fig. 5 shows a comparison of the values of solubility of H in Li determined here with the previous data of the pressure-composition isotherm [11]. The solubility constant under dilute solution of LiH in Li was correlated to the following equation:

$$K_{\text{Li–H}} = 0.480 \exp(-51.4[\text{kJ/mol-H}]/R_g T) \times [(\text{H/Li})/\text{Pa}^{0.5}]. \tag{11}$$

Comparatively close agreement was obtained with the extrapolation of the previous solubility that was determined at temperatures higher than 700 °C. This means that the Li surface on the upstream side absorbed hydrogen until its equilibrium value.

The large deviation in the diffusion coefficients between Moriyama et al. and ours may cause an uncertain thing in designing an Y trap to remove tritium from the IFMIF Li loop. There is possibility in that the discrepancy in diffusivity changes the tritium concentration

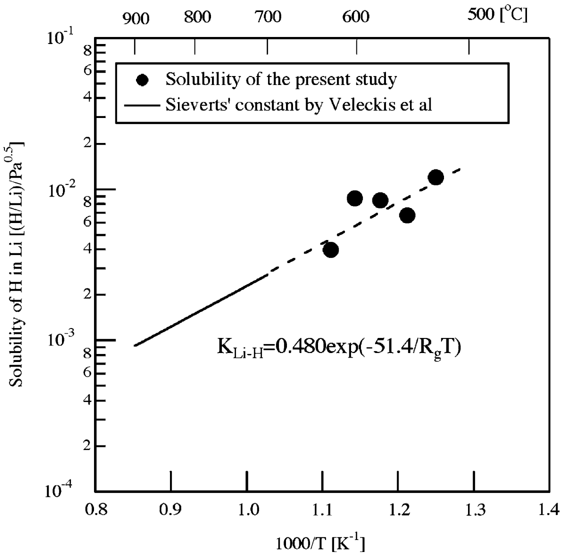

Fig. 5. Comparison of solubility between the present study and previous ones.

under a transient operation condition of the IFMIF Li loop. However, the steady-state tritium concentration, consequently tritium inventory, may not be affected by the discrepancy in diffusivity. On the other hand, the solubility by the present study was consistent with the extrapolation of previous solubility data under equilibrium. The tritium inventory under the steady-state IFMIF operation was deeply related with the solubility data. Therefore, there was no change in the estimation of tritium inventory of the IFMIF Li loop.

4. Conclusions

Hydrogen diffusivity in liquid Li was obtained by a capillary method between 500 °C and 650 °C. Our diffusivity data were correlated to $D_{\mathrm{Li-H}} = 1.38\exp(-162\,[\mathrm{kJ/mol}]/R_{\mathrm{g}}T)$. The data were consistent with one extrapolated from Alire's data. There was a large discrepancy in the activation energy of diffusivity between Moriyama's data and ours. The difference was discussed based on difference in the diffusion mechanism. There is high possibility in that the diffusion mechanism depends on the concentrations of hydrogen or other impurities. The effect of hydrogen dissociation and recombination on surface on the overall hydrogen permeation behavior was numerically investigated. The surface reaction could not explain the present hydrogen permeation behavior at all. Therefore the effect of the surface reaction was found to be negligibly small. Hydrogen solubility in liquid Li under dilute solution was consistent with the previous solubility data that were determined by Veleckis et al.

Acknowledgements

The authors would like to thank Dr Akio Suzuki of Tokyo University and Dr Hiroshi Nakamura of Japan Atomic Energy Research Institute for helpful discussions. This work has been performed under the NIFS LHD coordinated research (contract number NIFS05KOBF010).

References

[1] IFMIF International team, JAERI-Tech 2003-005, March 2003.
[2] H. Nakamura, B. Riccardi, N. Loginov, K. Ara, et al., J. Nucl. Mater. 329–333 (2004) 202.
[3] H. Nakamura, M. Ida, M. Sugimoto, T. Yutani, H. Takeuchi, Fus. Sci. Technol. 41 (2002) 845.
[4] M. Kinoshita, S. Fukada, et al., in: Proceedings ISFNT-7, Fus. Eng. Des., in press.
[5] R.E. Buxbaum, E.F. Johnson, Nucl. Technol. 49 (1980) 307.
[6] R.M. Alire, J. Chem. Phys. 65 (1976) 1134.
[7] H. Moriyama, K. Iwasaki, Y. Ito, J. Nucl. Mater. 191–194 (1992) 190.
[8] P.F. Adams, M.G. Down, P. Hubberstey, R.J. Pulham, J. Less Common Met. 42 (1975) 325.
[9] J.S. Murdy, R.M. Cotts, J. Chem. Phys. 48 (1968) 4938.
[10] E.N.C. Andrade, E.R. Dobbs, Proc. Roy. Soc. A211 (1952) 12.
[11] E. Veleckis, E.H. Van Deventer, M. Blander, J. Phys. Chem. 78 (1974) 1933.